# 13.5 THE STRUCTURE, EVOLUTION AND CLOUD PROCESSES OF A COLORADO UPSLOPE STORM AS SHOWN BY PROFILING RADIOMETER, RADAR AND TOWER DATA

Paul H. Herzegh*[1], Scott Landolt[1], and Tim Schneider[2]

[1]National Center for Atmospheric Research, Boulder, CO 80307
[2]NOAA/ERL/ETL, Boulder, CO 80305

## 1. INTRODUCTION

In their simplest form, upslope cloud and precipitation systems on the eastern flank of the Rocky Mountains typically bear a two-level vertical structure. Near the surface, the incursion of arctic air is marked by a stable, cool east or northeast flow. The arctic air may be as shallow as tens of m at its leading edge, and as deep as several km farther downslope. Atop these easterlies lies a second zone comprised of deeper westerlies. The stability, moisture content and depth of both layers exert strong controls on the effectiveness of orographic and synoptic lifting in the development of cloud and precipitation.

Observations made in the Boulder, Colorado, area on 4 March 2003 provide an opportunity to examine the structure of both upslope layers in relation to the evolution of cloud and precipitation within the system. Several key data sources supplement the operational surface, NEXRAD and NWS sounding data sets available for this study. These are

- a Radiometrics 12-channel microwave radiometer operated in Boulder by NCAR, yielding vertical profiles of temperature, water vapor and cloud liquid,
- the NOAA/ETL 2-channel K-band radiometer located in Erie, CO, yielding column-integrated measurements of water in vapor and liquid form,
- the NOAA/ETL K-band GRIDS prototype cloud profiling radar, also located in Erie, and
- *in situ* data obtained using the 300 m tower at NOAA's Boulder Atmospheric Observatory (BAO) in Erie, CO.

This work, a companion to the paper by Rasmussen and Ikeda (2003), seeks to document the physical processes active in this upslope case. An important further objective is to explore the meteorological value of temperature, relative humidity and liquid water profiles measured through the system by the 12-channel microwave radiometer. This latter goal lays the groundwork for planned use of the instrument in subsequent studies of low-level cloud and fog associated with ceiling and visibility aviation hazards in the NE U.S.

## 2. METEOROLOGICAL OVERVIEW

Early on 4 March 2003, the leading edge of a broad arctic airmass entered NE Colorado. Throughout the day it plunged southward through the central U.S. plains under the influence of a Canadian surface high, bringing NE surface winds with an upslope trajectory

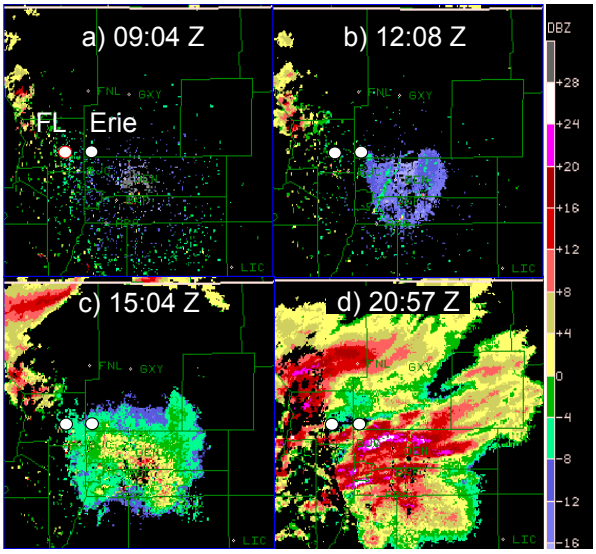


Figure 1. *Denver NEXRAD reflectivity scans at 0.5 deg elevation during the evolution of upslope precipitation in the Boulder/Denver area. (a) Clear air returns prior to arrival of the arctic air. (b) Reflectivity in the supercooled stratiform cloud within the low-level easterly upslope flow during the Boulder/Denver freezing drizzle event. (c) Stronger returns associated with light snow after the development of ice-phase processes in the upslope cloud. (d) Seeder-feeder precipitation resulting from the introduction of snow trails derived from generating cells within the westerlies above the low-level upslope cloud. In a), 'FL' marks the Foothills Lab location of the Radiometrics 12-channel microwave radiometer, and 'Erie' marks the location of the NOAA/ETL 2-channel microwave radiometer and the NOAA/ETL GRIDS K-band vertically-profiling radar.*

and (by about 10 Z) shallow near-surface upslope cloud bounded on the west by the Colorado front range. Although very little measurable precipitation was derived from the upslope system, freezing drizzle persisted in the Denver-Boulder region roughly over the period 11-16 Z, yielding significant icing of aircraft on the ground at Denver-area airports and strongly glazing commuters' automobile windshields.

A sequence of NEXRAD scans (Fig. 1) illustrates the 12-hour evolution of precipitation from shallow, freezing drizzle to snow derived from a seeder-feeder relationship between glaciated cloud in the westerlies aloft and liquid-bearing stratiform upslope cloud near the surface. While the low-level stratiform echoes in Figs. 1b and 1c were largely stationary, the strong reflectivity features associated with the trails in Fig. 1d moved from WNW to ESE .

* *Corresponding author address*: Paul H. Herzegh, NCAR, P.O. Box 3000, Boulder, CO 80307;
Email: herzegh@ucar.edu

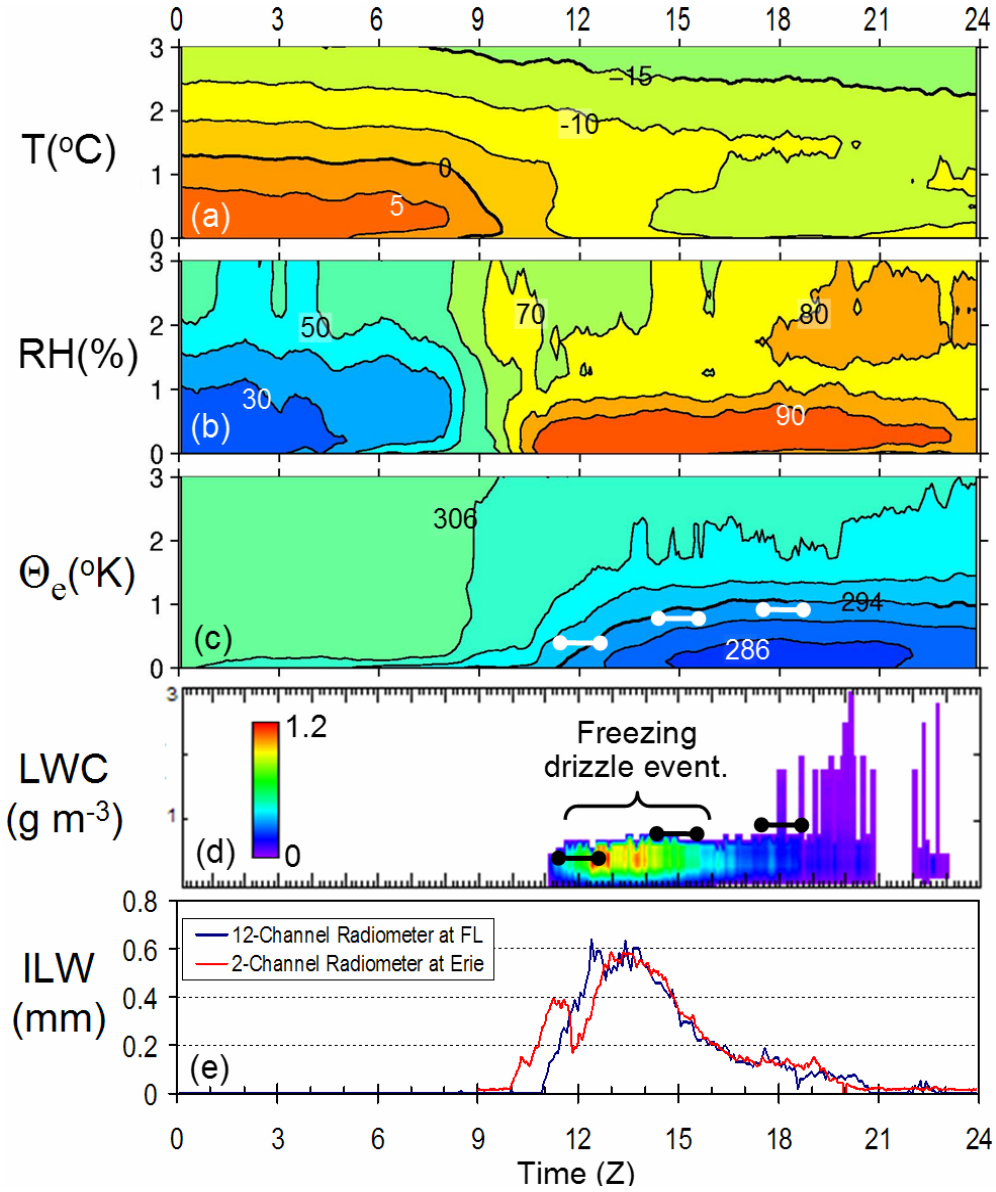


Figure 2. *(a)-(d) Time-height section of temperature, relative humidity, equivalent potential temperature and cloud liquid water content obtained by the Radiometrics 12-channel microwave radiometer located at Foothills Lab in Boulder (marked FL in Fig. 1). Estimated NEXRAD echo top heights are shown by the white and black bars in (c) and (d) respectively. (e) Time series of column-integrated liquid water (ILW) from the Radiometrics system and the NOAA/ETL 2-channel microwave radiometer.*

## 2. OBSERVATIONS OF SYSTEM STRUCTURE

The thermodynamic structure of the upslope system was examined through measurements from a vertically-pointing Radiometrics TP/WVP-3000 12-channel microwave profiling radiometer located at NCAR's Foothills Lab in Boulder (shown as FL in Fig. 1). The radiometer yields continuous (5-min interval) profiles of temperature, water vapor and cloud liquid water (Solheim *et al*., 1998; Ware *et al.*, 2003). While the profiles extend through the upper troposphere, we limit analysis to the lower levels in this case. Temperature profiling by the instrument is accomplished through neural net inversion of brightness temperatures ($T_b$) obtained from 7 microwave frequencies from 51 to 59 GHz on the flank of the 60 GHz oxygen resonance line. Water vapor profiles are derived through inversion of $T_b$ values at 5 frequencies from 22 to 30 GHz associated with the water vapor resonance peak at 22.2 GHz. Liquid water profiles are derived from $T_b$ values within both ranges. The neural net inversion process derives vertical profiles from observed $T_b$ values through use of an extensive training data set comprised of past Denver soundings

and their corresponding forward-modeled $T_b$ values.

The accuracy of derived profiles can be reduced by precipitation particles large enough to cause backscattering of upwelling microwave radiation from the surface. In the present case, the extremely light precipitation observed (drizzle and light snow) should not have had a significant effect. Accumulation of precipitation on the instrument's window surface was prevented through use of a high-power blower unit.

Sections of temperature and relative humidity in Figs. 2a-b show marked cooling and moistening below about 1.5 km altitude associated with the arrival of the arctic air between 9 and 12 Z. The moistening shown above 1.5 km after 17 Z coincides with the influx of seeder cloud and precipitation trails shown in Fig. 1d, which began about that time. A vertical section showing the low-level stratiform upslope cloud and the overlying seeder cloud cells carried via westerly flow aloft is shown by the NOAA/ETL GRIDS K-band vertically-profiling radar reflectivity data given in Fig. 3 below.

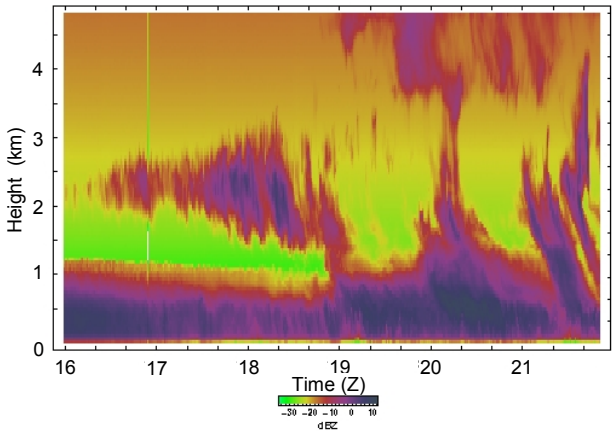


Figure 3. *Time-height section of reflectivity from the NOAA/ETL GRIDS K-band prototype radar located at the Erie site. The stratiform upslope cloud is seen below about 1.3 km agl. Mid-level cloud and snow trails are seen to originate above about 1.5 km agl.*

The arrival of the low-level arctic air is best shown by the section of equivalent potential temperature ($\theta_e$) in Fig. 2c. These data suggest that the leading edge of the arctic airmass took the form of a shallow wedge beneath about 0.3 km that arrived at FL between 8 and 9 Z. Arrival of much deeper arctic air began between 10 and 11 Z. The wedge-like leading edge shown above yields qualitative agreement with the timing of temperature shifts shown in Fig 4 measured by the NOAA/ETL 300 m Boulder Atmospheric Observatory (BAO) tower located 20 km east of the FL site.

The section of liquid water content (LWC) in Fig. 2d shows that the stratiform upslope cloud, though quite shallow, carried significant cloud liquid. Peak LWC estimates appear quite high, reaching about 1.1 g $m^{-3}$ in limited regions, with broader areas in the 0.6 to 0.8 g $m^{-3}$ range. This LWC feature coincides well with the period of freezing drizzle across the Boulder-Denver area, and diminishes as evidence of ice-phase processes (*e.g.*,

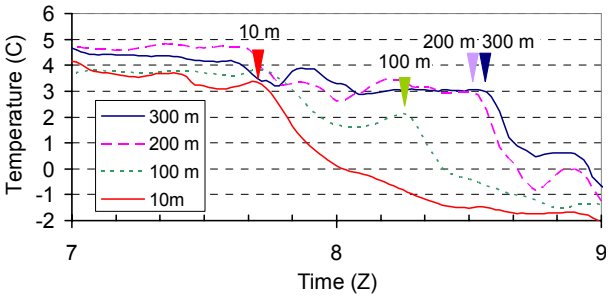


Figure 4. *Time series of temperature measurements at four levels on the BAO tower located 20 km east of the Boulder FL site. The temperature drop associated with the arrival of the arctic air occurred roughly 50 min earlier at 10 m agl than at 200 and 300 m agl.*

the occurrence of light snow and rapid increases in NEXRAD reflectivities) appear. The occurrence of high LWC, very low radar reflectivity, a single-layer cloud structure with relatively warm (~ -10 °C) cloud top temperatures, and persistent freezing drizzle are all clearly consistent with coalescence growth.

While individual peak LWC's measured by the profiling radiometer could in certain circumstances be in error by as much as 20-40%, the column-integrated liquid water (ILW) measurements shown in Fig. 2e further confirm the presence of a very significant peak in liquid water associated with the freezing drizzle event. The excellent agreement shown here between two independent radiometers (the NOAA/ETL system and the Radiometrics system) sited within 20 km of each other strongly supports the viability of ILW measurements in this case. Good results are in large part attributable to rigorous calibration of both systems and the lack of interfering precipitation, which can bias the microwave $T_b$ measurements. We thus expect that the accuracy of the ILW measurements meets the expectation of 10-20% cited by Westwater (1997).

## 3. SUMMARY AND DISCUSSION

Cloud Structure and Processes

The cloud structure and precipitation characteristics identified in this initial analysis of the 4 March upslope case define three stages of cloud function.

The first stage (roughly 11 to 14 Z) marks a period of coalescence growth associated with shallow single-layer upslope cloud that was strongly stratiform, supercooled throughout its depth, and ice-free. Cloud was essentially limited to the low-level layer containing the arctic air, with ceilometer-indicated cloud base at or below 100 m agl. Cloud top height is uncertain, but is likely bounded by the NEXRAD echo tops of ~ 0.4 km agl and the 1.2 km top of the moist layer shown by the Denver 00 Z sounding. Despite the shallow depth of the cloud, coalescence processes yielded a ~ 4-5 h period of freezing drizzle heavy enough to produce engine-damaging ice buildups on taxiing aircraft at Denver International Airport and a heavy glaze on commuters' automobile windshields. There was little if any evidence of a significant ice-phase process in the cloud during this stage. NEXRAD radar returns from the stratiform

cloud and drizzle during this period were low in reflectivity (generally < 0 dBZ), quite featureless in the horizontal, and capped at heights of about 0.4 to 0.8 km.

Column-integrated liquid water (ILW) in the first-stage cloud was measured independently by two microwave radiometers in the Boulder area and reached a peak of about 0.6 mm. The LWC derived from the profiling radiometer reached peaks from 0.6 to 1.1 g $m^{-3}$. Both the ILW and LWC values are consistent with a liquid water cloud supporting coalescence, and both are clearly inconsistent with a stratiform cloud supporting an ice-phase process. As shown in Fig. 2e, path integrated liquid water rose sharply with the arrival of the upslope cloud and maintained near-peak values during the freezing drizzle event.

The second stage (roughly 14 to 18 Z) marks the onset of significant ice-phase influences in the shallow upslope cloud. Here, the freezing drizzle began to transition to light snowfall, and NEXRAD reflectivities began a marked increase to peak values in the 5-10 dBZ range and greater. Integrated cloud liquid water began a steady decline from near-peak values to roughly 0.15 mm. The corresponding decline of ILW, transition from drizzle to light snow, and rise of radar reflectivity from very low to more moderate values suggests that depletion by growing ice particles is the mechanism that is responsible for the removal of liquid water. This is consistent with the findings in other Colorado storms by Rasmussen et al. (1995) and Politovich et al. (1995). Returns from the NOAA GRIDS prototype radar showed the occurrence of a second cloud layer within the westerlies at 2 km agl and above displaying a clear cell and trail structure resulting in seeding of the lower-level cloud by ice from above. Seeding of this sort is likely the key factor responsible for the introduction of ice into the lower stratiform cloud, and was thus the likely catalyst for each of the key changes associated with stage 2, *i.e.* the transition from drizzle to light snow, the increased NEXRAD reflectivities and the steady reduction of cloud liquid water by scavenging.

The third stage (roughly 18 to 24 Z) represents a seeder-feeder ice-phase cloud process in mature form. Well-defined precipitation trails originating from generating cells embedded in the westerly flow above the arctic air impinged upon the low-level stratiform upslope cloud within the arctic air and yielded the peak reflectivities seen for the day – in the 20-30 dBZ range.

Profiling Radiometer Performance

This initial application of the profiling radiometer system within NCAR has yielded encouraging interim results relative to qualitative studies of low-level thermodynamic and cloud microphysical structures. Our work has not addressed detailed, longer-term comparison with RAOBS or other *in situ* sounding systems. The reader is referred to work by Güldner and Spänkuch (2001) and Liljegren (2001) for more systematic evaluations under other conditions.

In brief, however, we find the overall thermodynamic structure shown in Figs. 2a-c to be quite consistent with expectations based upon past study, and quite informative relative to needs to differentiate the bulk temperature and humidity characteristics of one airmass versus another. The availability of continuous (rather than intermittent) sounding observations is a particularly valuable asset where isentropic analysis is the goal. The very close agreement between the ILW time series measured independently by the Radiometrics and NOAA/ETL systems is an encouraging indication that optimum bulk accuracy of 10-20% may be achievable here.

**Acknowledgements**

This research is in response to requirements and funding by the Federal Aviation Administration (FAA). The views expressed are those of the authors and do not necessarily represent the official policy or position of the FAA. The authors thank Matt Tryhane of NCAR for processing help and Dan Wolfe of NOAA/ETL for providing the BAO Tower data.

**REFERENCES**

Güldner, J. and D. Spänkuch, 2001: Remote sensing of the thermodynamic state of the atmospheric boundary layer by ground-based microwave radiometry. *J. Atmos. Ocean. Tech*., 18, 925-933.

Liljegren, J., E. Clothiaux, S. Kato, B. Lesht, 2001: Initial evaluation of profiles of temperature, water vapor and cloud liquid water from a new microwave profiling radiometer. *Proc. 5th Symp. Int. Obs. Systems*, AMS, Boston.

Politovich, M. K. and B. C. Bernstein, 1995: Production and depletion of supercooled liquid water in a Colorado winter storm. *J. Appl. Meteor.*, 34, 2631-2648.

Rasmussen, R. M. and K. Ikeda, 2003: Radar observations of a freezing drizzle case in Colorado. *Proc. 31st Conf. on Radar Meteor*. (this volume), AMS, Boston.

Rasmussen, R. M., B. Bernstein, M. Murakami, G. Stossmeister and J. Reisner, 1995: The 1990 Valentine's Day arctic outbreak. Part I: Mesoscale and microscale structure and evolutions of a Colorado front range shallow upslope cloud. *J. Appl. Meteor.*, 34, 1481-1511.

Solheim, F., J. Godwin, E. Westwater, Y. Han, S. Keihm, K. Marsh, R. Ware, 1998: Radiometric profiling of temperature, water vapor, and liquid water using various inversion methods. *Rad. Sci*., 33, 393-404.

Ware, R., R. Carpenter, J. Güldner, J. Liljegren, T. Nehrkorn, F. Solheim and F. Vandenberghe, 2003: A multi-channel radiometric profiler of temperature, humidity and cloud liquid. *Rad. Sci.*, (in press).

Westwater, E., 1997: Remote sensing of tropospheric temperature and water vapor by integrated observing systems. *Bull. Amer. Met. Soc.*, 78, 1991-2006.